AIP Applied Physics Letters

Collective flow dynamics across a bacterial carpet: Understanding the forces generated

Yi-Teng Hsiao, Jing-Hui Wang, Kuan-Ting Wu, Jengjan Tsai, Cheng-Hung Chang, and Wei-Yen Woon

Citation: Applied Physics Letters **105**, 203702 (2014); doi: 10.1063/1.4902111
View online: http://dx.doi.org/10.1063/1.4902111
View Table of Contents: http://scitation.aip.org/content/aip/journal/apl/105/20?ver=pdfcov
Published by the AIP Publishing

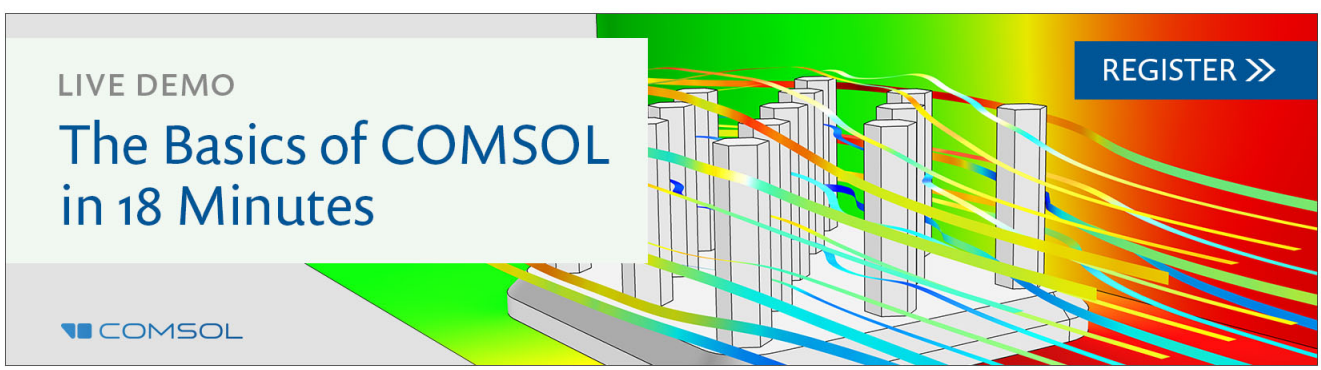

Collective flow dynamics across a bacterial carpet: Understanding the forces generated

Yi-Teng Hsiao,[1] Jing-Hui Wang,[1] Kuan-Ting Wu,[1] Jengjan Tsai,[2] Cheng-Hung Chang,[2] and Wei-Yen Woon[1,a)]
[1]*Department of Physics, National Central University, Jungli 32054, Taiwan*
[2]*Institute of Physics, National Chiao Tung University, Hsinchu 300, Taiwan*

(Received 15 July 2014; accepted 7 November 2014; published online 18 November 2014)

Bacterial carpets consist of randomly anchored uni-polar-flagellated sodium-motive bacterial matrix are prepared by flow deposition. Collective flow dynamics across the bacterial carpets are probed with optical tweezers-microsphere assay. Around the center of a uniform bacterial cluster, collective forces that pull microsphere towards carpet surface are detected at a distance of 10 μm away from carpets. At sodium-motive driving over a critical value, the force magnitudes increase abruptly, suggesting a threshold-like transition of hydrodynamic synchronization across bacterial carpet. The abrupt force increase is explained in term of bifurcation to phase synchronization in a noisy nonlinearly coupled rotor array mediated by hydrodynamic interactions. © *2014 AIP Publishing LLC*.
[http://dx.doi.org/10.1063/1.4902111]

Emergent collective dynamics in many-body self-propelled particle (SPP) system is a ubiquitous phenomenon in nature.[1,2] Among all SPP systems, bacterium is probably the most thoroughly studied due to its biological importance.[3] Under high bacterial concentration condition or at close proximity to surface, the swimming behaviors of bacteria have been found to alter dramatically due to complex interactions with neighbors and boundaries.[4–7] The rich phenomena arise from collective interactions between SPP and boundaries are interesting fluid dynamics issues to be explored. Recently, collective flow dynamics across bacteria attached surfaces, namely, bacterial carpets, has been experimentally and theoretically studied.[8–11] Synchronization of flagellar motions through hydrodynamic coupling has been suggested. Whether there exists a threshold in coupling strength above which onset of synchronization take place is still an open issue and is yet to be verified experimentally. Besides, the effect of phase synchronization among bacterial flagellar motions on the surrounding fluid has not been well addressed.

In this work, we investigate the above issues by employing a bacterial carpet formed by anchored uni-polar-flagellated bacterium mutant strain *Vibrio alginolyticus* (NMB136). The bacteria strains were kind gifts from C. J. Lo and M. Homma.[12] Standard motility protocols were used for incubation of the bacteria.[13] Contrary to wild type *V. alginolyticus* (VIO5) which can swim forward or backward, switched with a large angle flicking,[14–16] the mutant strain NMB136 could only swim forward due to lack of clockwise (CW) flagellar rotation (Fig. 1(a)). After cell culture, dense bacteria containing solution (final concentration $\sim 10^{10}$ cell/μl) is injected into a custom made of 180 μm high, poly-L-lysine pre-treated microchannel to result in a bacterial carpets covered surface for experiment observation. The density of bacterial carpet appears to be quite uniform within each domain with size less than 10 μm (site *A* in inset of Fig. 1(b)). Between each domain, there are regions with obviously lower bacterial density (e.g., site *B* in Fig. 1(b)). Most bacteria are observed to attach on substrate with small inclined angle, probably due to the downward force imposed on swimming bacteria near boundary (Fig. 1(c)).[5] Schematic plot shown in Fig. 1(d) illustrates the typical spatial distribution of bacterial carpet. As a simplified model, we can treat the thrust exerted from rotating flagellum of an anchored cell to be equivalent to the thrust from rotating rotor anchored on substrate, similar to the picture in previous works.[10,11]

It is known that measuring rotation rate of the rare tethered cell among bacterial carpet could provide the individual flagellar rotation rate information by considering the difference in Stokes drag between flagellum and cell body.[17] As the cell body is much more massive than flagellum, coupling between the cell body rotation to nearby flagellum motion can be neglected. To measure the rotation rate of tethered cell among a dense bacterial carpet, we use a high speed CCD camera (CR450x2, Optronis) with 1 KHz frame rate. Typical images and trajectories of tethered cell body are shown in Figs. 2(a) and 2(b). As *V. alginolyticus* belongs to the category of sodium-motive cells, precise rotation rate tuning by Na^+ concentration control in the motility buffer is possible, as shown in the histograms in Fig. 2(c). Fig. 2(d) shows the measured swimming speed and corresponding rotation rate versus Na^+ concentration for each case. The rotation rate shows linear increase trend under Na^+ concentration range of 50 mM–300 mM. It is therefore expected that the thrusts exerted by a rotating flagellum of an individual anchored bacterium to surrounding medium also increase linearly as Na^+ concentration increases.

Implementing an optical tweezers to above system allows us to measure the collective flow and forces across bacterial carpets. Fig. 3(a) shows the schematic plot of experiment setup. A focused 633 nm He-Ne laser is introduced into the bacterial carpet micro-channel through 60× oil immersion microscope objective (Olympus UPLAPO, N. A. = 1.25). A 2-μm particle is trapped at the laser focus at

a)Author to whom correspondence should be addressed. Electronic mail: wywoon@phy.ncu.edu.tw.

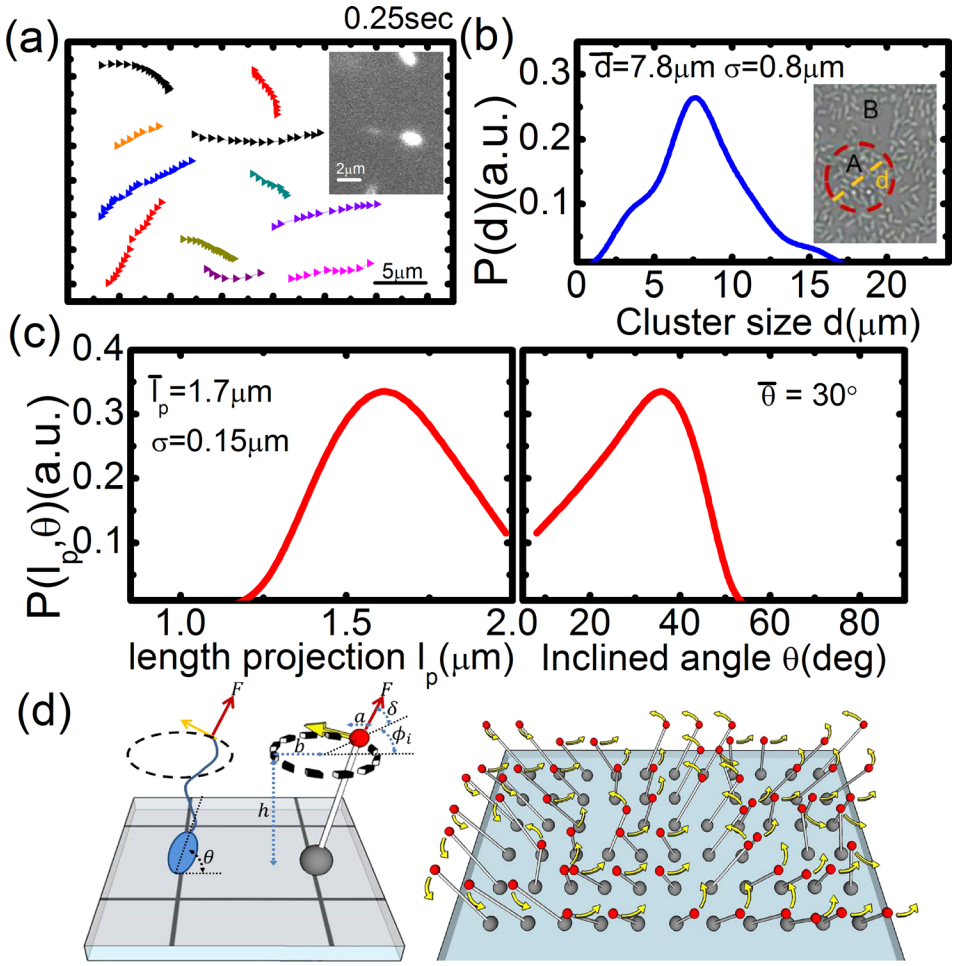

FIG. 1. (a) Typical trajectories for swimming mutant strain *V. alginolyticus* NMB136 under Na^+ concentration = 300 mM. Total time span is 0.25 s. The inset shows the dark field optical image of the uni-polar flagellated bacterium. (b) Distribution of bacterial carpet cluster size. Inset shows the optical image of carpet, with definition of cluster size d in region A, where the force measurement are conducted. Region B represents region with low density. (c) The histogram of inclined angle between cell body and substrate converted from cell body projection length measurement acquired with phase contrast optical microscopy. (d) Left column shows the simplified rotor model for anchored bacterium. The rotating flagellum exerts thrusts in tangential, normal, and vertical directions (f_t, f_n, f_z), where $f_{t,z,n} = \frac{\omega_{t,z,n}}{6\pi\eta ab}$, with $\omega_{t,z,n}$ the component of rotation rate in respective direction. Definition of a (effective rotor size), b (radius of rotating span), h (rotor height), θ (inclined angle), and δ (angle between tangential and normal thrusts) are depicted in the schematic. The right column shows the schematic of bacterial carpet experiment system as anchored rotor matrix.

a location >10 μm away from bacterial carpet. We purposely restrain the measurement distance to above 10 μm away from carpet in order to alleviate the possibility of direct contact between tracer particle and flagellum. The force at each measuring location is then determined by continuously decreasing laser power until the tracer particle is no longer trapped at the laser focus.[18] It is noteworthy that the force directions and magnitudes may vary for different locations on carpet, due to the random nature of the carpet and existence of backflow associated with any outward/inward flow. The data (each data point is average of more than ten measurement runs across ten different clusters) represent the force measurement result at the central regions across uniform domains with average size less than 10 μm (e.g., site A in Fig. 1(b)). More detail about the assay can be found in the supplementary material.[13] Figure 3(b) shows the forces measured at various distances from bacterial carpets. A vertical force pulling tracer particle towards bacterial carpet surface is measured across the bacterial carpet. The magnitudes of the forces decrease as distances from bacterial carpet increase. Increase of Na^+ concentration in the motility buffer to over 100 mM leads to significant increase in force magnitude.

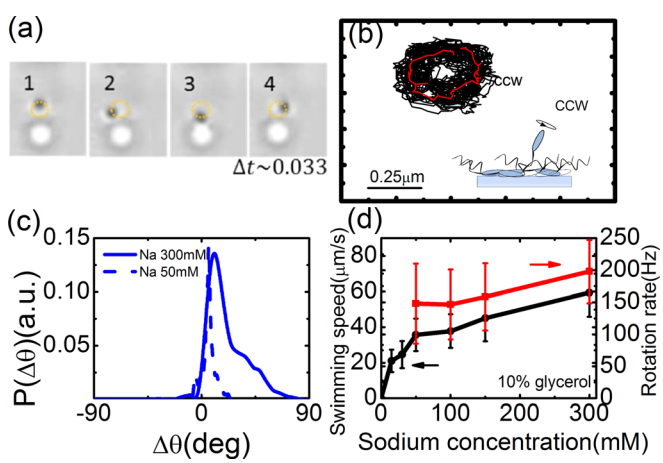

FIG. 2. (a) Typical images of cell body rotation. (b) Typical cell body trajectories (15 s) of tethered cell among bacterial carpet. Stable CCW motion is found for the mutant strain *V. alginolyticus* NMB136. The inset shows the schematic side view. 300 mM Na^+ concentration with 10% glycerol mixed motility buffer is used for the above two cases. (c) Histograms of angle change in 10 s time span for rotating tethered cell under 50 mM and 300 mM Na^+ concentration. (d) Swimming speed (black symbol) and flagellar rotation rate (red symbol) versus Na^+ concentration. Linear relation holds between swimming speed and flagellar rotation above Na^+ concentration >50 mM.

In boundary free fluidic environment, the far field flow generated from a swimming single polar-flagellated bacterium with counterclockwise (CCW) flagellar rotation can be modeled as a positive ("pusher") force dipole. Physically, the anchoring of cell body leads to vanishing of the forward flow field for a force dipole model due to symmetry breaking, and can be regarded as an anchored force monopole. The close proximity of the surface boundary inevitably results in backflowing of the towards-surface flow components in the flow

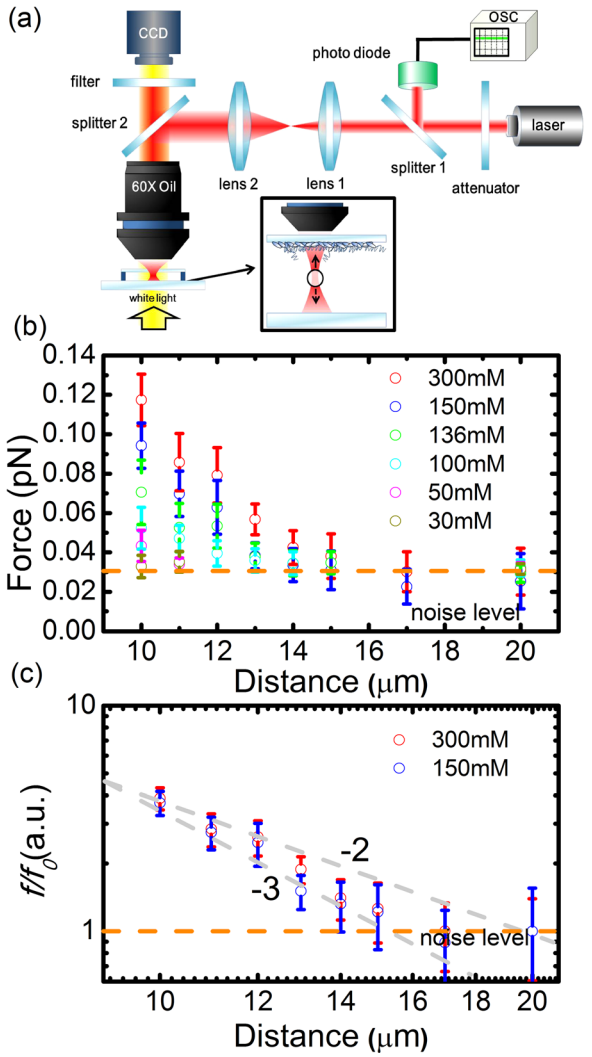

FIG. 3. (a) Schematic setup of the optical tweezers-microsphere assay. Bacterial carpet is formed primarily on the polylysine pretreated top cover slides of the 180-μm high custom made micro-channel. (b) The measured force magnitude (pulling towards surface) with respect to distance from carpets, under different Na^+ concentrations. (c) The reduced force magnitude f/f_0 (with f_0 the average magnitude of noise level) (Na^+ concentration >136 mM). The slope $=-3$ and -2 dashed curves are drawn as guiding to eyes.

field. Moreover, in bacterial carpet condition, the cell to cell distance between each bacterium constitutes additional boundary condition that promotes bending of flow lines. Theoretically, considering an anchored rotor at a non-slip boundary, the hydrodynamic interaction (Blake-Oseen tensor) G should consists of a Stokeslet G_S from a force monopole, and an image system required for satisfying the no-slip boundary condition.[19] For measurement conducted at a distance far away from flagellum, the assumption of superposition of thrusts from anchored monopoles should give a r^{-2} scaling, while our experimental result gives a r^{-2} to r^{-3} scaling within the experimental data error bar. It is probable that the near field components may results in the observed deviation. Further clarification on the exact force scaling requires more elaborated simulation. Nevertheless, the above consideration suggests that the collective flow field from anchored bacterial matrix can be understood as a collective superposition of flow fields from anchored force monopoles and their associated image flow fields, mediated by hydrodynamic interactions. Furthermore, for an upright head-down cell attachment, collective pushing force is expected for CCW rotating flagellum. However, the experimental observation shows reversed directions. Nevertheless, if the inclined angle between the cell body and the substrate is less than 45°, the force experienced by the tracer particle should be reversed due to mass conservation. Experimentally, as the average inclined angles peak at 30° (cf. Fig. 1(c)), the collective flow direction reversal can be understood by the above scenario.

Similar to a non-linearly coupled rotor matrix in noisy environment,[20] we can describe the phase change rate ($\frac{d\Phi}{dt}$) of a rotor in a matrix by the following equation:[13,21,22]

$$\frac{d\Phi_i}{dt} = -\gamma\omega\sum_{j\neq i}\frac{1}{|r_{ij}|^3}\sin\left(\Phi_i - \Phi_j - \delta\right) + \Omega_i(t), \quad (1)$$

where $\delta = \tan^{-1}(\frac{\omega_t}{\omega_n})$, $\langle\Omega_i(t)\Omega_j(t')\rangle = 2D_r\delta_{ij}\delta(t-t')$, $D_r = \frac{k_bT}{6\pi\eta ab}$, and $\gamma = \frac{9ah^2}{2}$ are the angle between tangential and normal thrusts,[11] time correlation of random noises, rotational diffusion constant, and hydrodynamic coupling constant, respectively (cf. Fig. 1(a)). Typical values of $k_bT = 4\times10^{-21}$J, $\eta = 1.3\times10^{-3}$Pas, effective rotor size a$=0.1\,\mu$m, radius of rotating span b$=0.5\,\mu$m, and rotor height h$=5\,\mu$m are employed by considering the realistic conditions in our experiment (the reasons for the choice of parameters employed is documented in the supplementary material).[13] Bifurcation from a random phase to synchronized phase should occur if a critical parameter is tuned stronger across a threshold value. We define the effective hydrodynamic coupling parameter $\Delta = \frac{\gamma\omega}{d^3\sqrt{2D_r}}$, where d is the effective length scale of the synchronized cluster (averaged cluster size$=7.8\,\mu$m from Fig. 1(c)). Bifurcation to phase synchronization state occurs at $\Delta \geq 1$. In another word, by tuning the flagellar rotation rate ω to over a critical ω_c, bifurcation to a synchronized state is expected. Employing the above parameters, ω_c is estimated to be 151Hz for present case. Defining an order parameter $S = \langle\cos\phi\rangle$ similar to Uchida and Golestanian,[11] we expect to have $S \propto \sqrt{(\Delta - \Delta_c)}$, as shown by the dashed curve in Fig. 4.The symbols in Fig. 4 show the reduced force magnitude f/f_0 (with f_0 the average magnitude of noise level) exhibit an abrupt increase in magnitude at

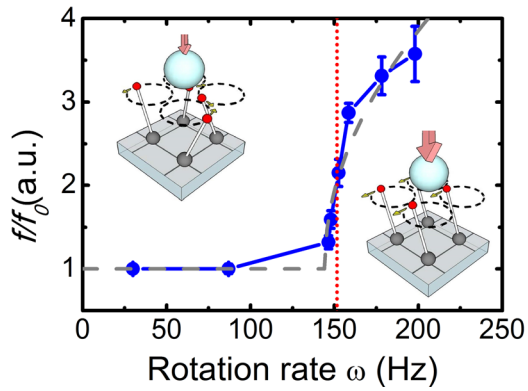

FIG. 4. The reduced force magnitude f/f_0 measured at 10 μm across bacterial carpet versus rotation rate ω. Insets show the figurative presentations of synchronization transition.

sodium-motive driving rotation rate ω (Na^+ concentration) over a critical value (around 150Hz).

The physics underlying the observation can be understood as follows. The rotation rate ω of a rotor in a matrix is a combined result of self-driving and superposition of thrusts from neighboring rotor. At higher sodium-motive driving rotation rate, each flagellum exerts stronger thrust to surrounding fluid, results in stronger hydrodynamic coupling between neighboring flagella, and leads to phase locking between each flagellar rotation. As the coupling gets stronger, synchronized cluster with higher flagellar rotation rate may be expected due to lower effective dissipation (cf. inset of Fig. 4). It consequently leads to stronger collective vertical flow detected by the tracer particle across the carpet. The observation is reminiscence of theoretical simulation by Uchida and Golestanian,[11] where reduction of noise level leads to more pronounced synchronization in rotor matrix. In this work, the effect of synchronization among flagellar motions on the surrounding flow field is further explored. Nevertheless, there remains other probable source of disorder in the system, namely, the disorder in distribution of flagellar rotation rate among the anchored bacteria.[23] In that case, a more smeared transition curve is expected. At this moment, we are not able to precisely point out which sources of disorder dominate in our system. Further clarification is expected after more theoretical simulation works and elaborated measurement around the transition point.

This work was supported by Ministry of Science and Technology of Taiwan under Contract No. MOST103-2112-M008-019-MY3. We gratefully acknowledge the facility support from Professor H. K. Tsao and NCUPHY biophysics core facility.

[1]J. Toner, Y. H. Tu, and S. Ramaswamy, Ann. Phys. **318**, 170 (2005).
[2]T. Vicsek and A. Zafeiris, Phys. Rep. **517**, 71 (2012).
[3]H. C. Berg, Phys. Today **53**(1), 24 (2000).
[4]Y. Sowa, H. Hotta, M. Homma, and A. Ishijima, J. Mol. Biol. **327**, 1043 (2003).
[5]A. P. Berke, L. Turner, H. C. Berg, and E. Lauga, Phys. Rev. Lett. **101**, 038102 (2008).
[6]W. R. DiLuzio, L. Turner, M. Mayer, P. Garstecki, D. B. Weibel, H. C. Berg, and G. M. Whitesides, Nature **435**, 1271 (2005).
[7]S. E. Spagnolie and E. Lauga, J. Fluid Mech. **700**, 105 (2012).
[8]N. Darnton, L. Turner, K. Breuer, and H. C. Berg, Biophys. J. **86**, 1863 (2004).
[9]M. J. Kim and K. S. Breuer, Small **4**, 111 (2008).
[10]Y. T. Hsiao, J. H. Wang, Y. C. Hsu, C. C. Chiu, C. J. Lo, C. W. Tsao, and W. Y. Woon, Appl. Phys. Lett. **100**, 203702 (2012).
[11]N. Uchida and R. Golestanian, Phys. Rev. Lett. **104**, 178103 (2010).
[12]Y. Magariyama, M. Ichiba, K. Nakata, K. Baba, T. Ohtani, S. Kudo, and T. Goto, Biophys. J. **88**, 3648 (2005).
[13]See supplementary material at http://dx.doi.org/10.1063/1.4902111 for experimental and theoretical calculation details.
[14]L. Xie, T. Altindal, S. Chattopadhyay, and X. L. Wu, Proc. Natl. Acad. Sci. U.S.A. **108**, 2246 (2011).
[15]S. Chattopadhyay, R. Moldovan, C. Yeung, and X. L. Wu, Proc. Natl. Acad. Sci. U.S.A. **103**, 13712 (2006).
[16]K. Son, J. S. Guasto, and R. Stocker, Nat. Phys. **9**, 494 (2013).
[17]L. Turner, R. J. Zhang, N. Darnton, and H. C. Berg, J. Bacteriol. **192**, 3259 (2010).
[18]M. Grimm, T. Franosch, and S. Jeney, Phys. Rev. E **86**, 021912 (2012).
[19]J. R. Blake, Proc. Cambridge Philos. Soc. **70**, 303 (1971).
[20]S. H. Strogatz, *Non-Linear Dynamics and Chaos* (Perseus, New York, 1994).
[21]R. Golestanian, J. M. Yeomans, and N. Uchida, Soft Matter **7**, 3074 (2011).
[22]Y. Kuramoto, *Chemical Oscillations, Waves, and Turbulence* (Springer, Berlin, 1984).
[23]N. Uchida and R. Golestanian, Europhys. Lett. **89**, 50011 (2010).